



Title of proposed experiment:

Measurement of the Astrophysical Rate of the $^{20}\text{Na}(p,\gamma)^{21}\text{Mg}$ Reaction

Name of group: DRAGON

Spokesperson for group: J.M. D'Auria / A.A. Chen

E-Mail address: dauria@sfu.ca

Fax number: (604)222-1074

Members of the group (name, institution, status, per cent of time devoted to experiment)

<u>Name</u>	<u>Institution</u>	<u>Status</u>	<u>Time</u>
J.M. D'Auria	Simon Fraser University	Professor	80%
A.A. Chen	Simon Fraser University	Research Associate	80%
S. Bishop	Simon Fraser University	Graduate Student	80%
L. Buchmann	TRIUMF	Research Scientist	30%
D. Hunter	Simon Fraser University	Research Associate	80%
A. Hussein	University of Northern British Columbia	Professor	80%
D.A. Hutcheon	TRIUMF	Research Scientist	60%
W. Liu	Simon Fraser University	Graduate Student	80%
A. Olin	TRIUMF	Research Scientist	30%
J. Rogers	TRIUMF	Research Scientist	80%
G. Roy	University of Alberta	Professor Emeritus	60%
F. Strieder	Ruhr-Universität Bochum	Research Scientist	20%
S. Theis	Ruhr-Universität Bochum	Graduate Student	60%



Start of preparations: 1997

Date ready: June 2001

Completion date: 2002

Beam time requested:

12-hr shifts ~ 50 Beam line/channel ISAC Polarized primary beam? No

The $^{20}\text{Na}(p,\gamma)^{21}\text{Mg}$ reaction is thought to be an integral part of the breakout process from the hot CNO cycle to the rp-process or NeNa cycle, leading to heavy element production in extreme astrophysical environments, such as novae and type I x-ray bursts. One of the breakout paths is the $^{15}\text{O}(\alpha,\gamma)^{19}\text{Ne}(p,\gamma)^{20}\text{Na}(p,\gamma)^{21}\text{Mg}$ reaction sequence. Our present understanding points to the radiative alpha-capture reaction as the key reaction in this series, but there is only sparse information on the $^{20}\text{Na}(p,\gamma)^{21}\text{Mg}$ reaction rate and hence its contribution to the breakout process is poorly understood. No direct measurements of the $^{20}\text{Na}(p,\gamma)^{21}\text{Mg}$ reaction have been performed to date, and spectroscopic information for levels in ^{21}Mg has been obtained from only one previous study.

We therefore propose to measure the rate of the $^{20}\text{Na}(p,\gamma)^{21}\text{Mg}$ reaction using the DRAGON facility using ^{20}Na beams in the energy range $E_{cm} = 0.13$ to 0.8 MeV/u, which will cover the $^{20}\text{Na} + p$ resonances in ^{21}Mg considered to be important for explosive nucleosynthesis in both novae and x-ray bursts.

Experimental area

This experiment will be performed using the DRAGON facility in the ISAC experimental hall.

Primary beam and target (energy, energy spread, intensity, pulse characteristics, emittance)

The primary production beam will be the 500 MeV proton beam from the TRIUMF cyclotron.

Secondary channel

Secondary beam (particle type, momentum range, momentum bite, solid angle, spot size, emittance, intensity, beam purity, target, special characteristics)

The secondary beam required is ^{20}Na with the highest intensities achievable and with energies from $E_{cm} = 0.13$ to 0.8 MeV/u. Useful experimental results can be obtained with intensities $> 10^8$ ions per second. In addition, several stable heavy ion beams such as ^{20}Ne and ^{21}Ne will also be needed to finalize the tuning of the DRAGON facility.

TRIUMF SUPPORT:

Continued infrastructure support from TRIUMF for DRAGON at ISAC, including assigned personnel.

NON-TRIUMF SUPPORT

NSERC DRAGON Project Grant (J.M. D'Auria et al.), submitted to NSERC in November 2000 for 3-year support request.

This experiment does not introduce any additional safety hazards beyond those covered under the normal operation of the DRAGON and ISAC facilities. Safety procedures for the operation of DRAGON are in development.

1 Scientific Justification

1.1 The $^{20}\text{Na}(p,\gamma)^{21}\text{Mg}$ Reaction and Breakout to the rp-Process

In the continuing quest to understand the connection between nuclear processes and stellar evolution and phenomena, one branch of nuclear astrophysics that has received considerable attention in recent years from observational, theoretical, and experimental fronts is the study of explosive nucleosynthesis, which focuses primarily on the nuclear processes that drive stellar explosions, such as nova explosions and type I x-ray bursts. While quiescent nuclear burning, exemplified by the pp-chains and the CNO-cycles, tends to happen relatively slowly, in stellar explosions the temperature and density are extreme enough so that the nuclear reactions occur on a time-scale that is faster than the typical lifetimes of the β -unstable isotopes. As a result, in explosive nucleosynthesis, reactions involving unstable nuclei can become important, resulting in significant consequences for both energy and element production.

Type I x-ray bursts and novae are examples of binary stellar sites where explosive nucleosynthesis can happen as a result of accretion of material onto the degenerate partner. According to current models, the energy generation and nucleosynthesis at temperatures of $T \sim 0.4$ GK are determined by the Hot-CNO cycles [1]. In the case of x-ray bursts, these cycles by themselves are insufficient to account for the observed energy output. As the temperature and density on the surface of the accreting star increase, however, α -particle and proton capture reactions on the Hot-CNO nuclei become faster than the corresponding β^+ decays and, in x-ray bursts where the surface gravity is high, the star may then break out of the Hot-CNO to the rp-process, providing a way to enhance the rate of energy generation, trigger the subsequent explosion, and produce heavier elements up to roughly $A = 100$. Based on present nuclear physics information, the initial breakout flux becomes significant at $T = 0.6$ GK and runs primarily through the reaction sequence $^{15}\text{O}(\alpha,\gamma)^{19}\text{Ne}(p,\gamma)^{20}\text{Na}(p,\gamma)^{21}\text{Mg}\dots$ [2]. At higher temperatures ($T \geq 0.8$ GK), another path to the rp-process becomes available to the star through the sequence $^{14}\text{O}(\alpha,p)^{17}\text{F}(p,\gamma)^{18}\text{Ne}(\alpha,p)^{21}\text{Na}\dots$, with the $^{18}\text{Ne}(\alpha,p)^{21}\text{Na}$ reaction providing the bridge to $A \geq 20$ (see Figure 1) [2]. The contribution of these reactions to the total reaction flux through this mass region depends on their cross sections under extreme stellar conditions, and presently these cross sections are poorly known for most cases. Only recently have first experiments been carried out at various laboratories, and many further reaction studies have been already approved as experiments to be performed with short-lived beams at ISAC and other facilities.

With regards to the initial path mentioned above, the first two reactions of this first sequence, $^{15}\text{O}(\alpha,\gamma)^{19}\text{Ne}$ and $^{19}\text{Ne}(p,\gamma)^{20}\text{Na}$, have traditionally been considered the key reactions that determine the overall breakout flux to the rp-process via this path. This is justified, since these reactions, strictly speaking, are the ones that actually bridge the CNO mass region to $A > 20$. While the third reaction in the sequence, $^{20}\text{Na}(p,\gamma)^{21}\text{Mg}$, may be regarded as the first reaction of the rp-process, the viability of this path leading up to ^{20}Na as the main breakout sequence clearly depends also on the rate of the $^{20}\text{Na}(p,\gamma)^{21}\text{Mg}$ reaction. Based on the present reaction rates, one should note that the nucleosynthesis material will not be recycled back into the CNO region once ^{20}Na is reached, implying therefore that the $^{20}\text{Na}(p,\gamma)^{21}\text{Mg}$ reaction will not prevent the star from leaving the Hot-

CNO cycles through the path initiated by the $^{15}\text{O}(\alpha, \gamma)^{19}\text{Ne}$ reaction. Nevertheless, the degree of competition between this path and the one featuring the $^{18}\text{Ne}(\alpha, p)^{21}\text{Na}$ reaction will depend critically on the rate of the $^{20}\text{Na}(p, \gamma)^{21}\text{Mg}$ reaction rate at the relevant temperatures.

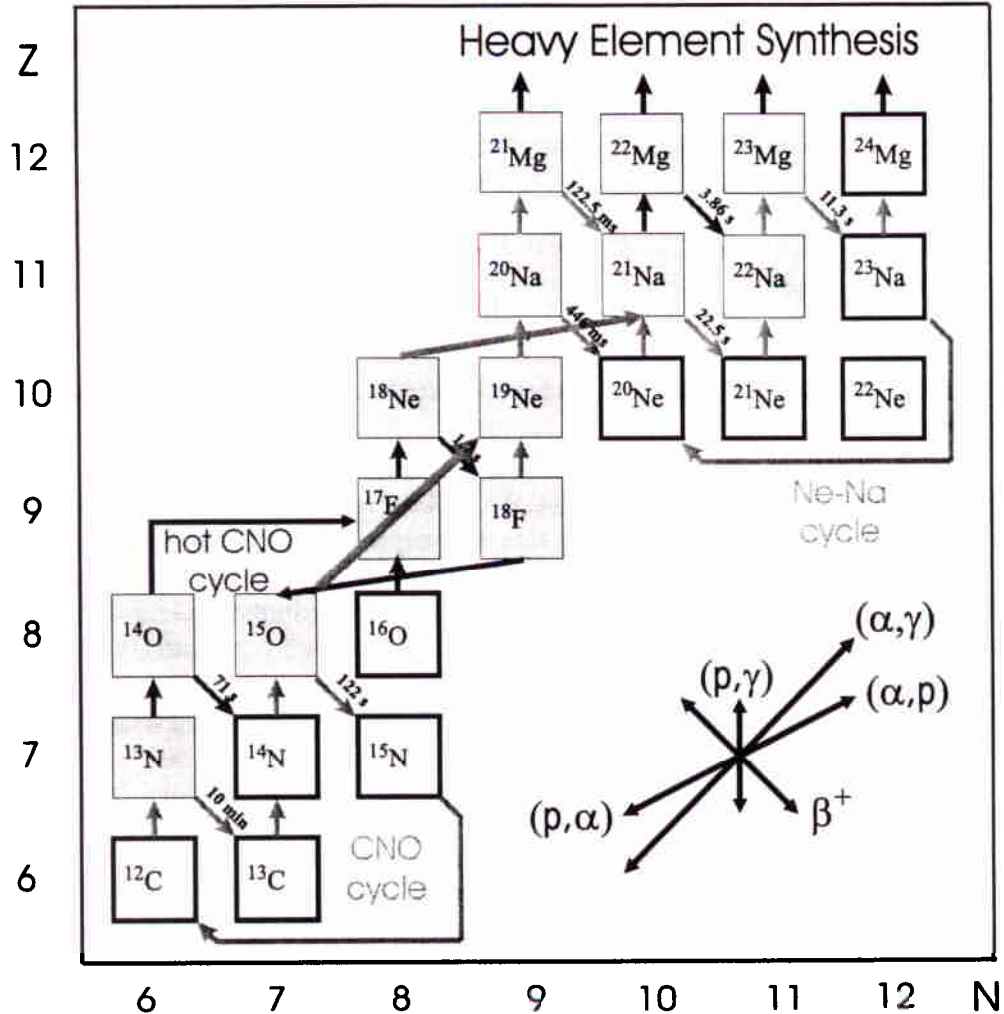


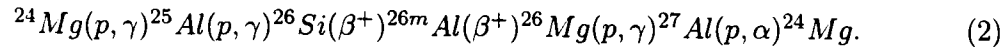
Fig. 1 Reaction networks in the Hot-CNO cycles and possible breakout paths.

1.2 $^{20}\text{Ne}(p, \gamma)^{21}\text{Mg}$ and the NeNa Cycles in Nova Explosions

While breakout from the Hot-CNO cycles supplies the energy trigger for x-ray bursts, our present understanding of explosive nucleosynthesis in novae (where the accreting star is a white dwarf instead of a neutron star) indicates that the temperatures reached are too low for breakout to happen. For ONeMg novae, the energy sources are instead the NeNa and MgAl cycles [1],

$$^{20}\text{Ne}(p, \gamma)^{21}\text{Na}(p, \gamma)^{22}\text{Mg}(\beta^+)^{22}\text{Na}(p, \gamma)^{23}\text{Mg}(\beta^+)^{23}\text{Na}(p, \alpha)^{20}\text{Ne} \quad (1)$$

and



The nucleosynthesis resulting from hydrogen burning in these cycles depends on the amount of seed ${}^{20}\text{Ne}$ and ${}^{24}\text{Mg}$ present initially on the white dwarf. Note however that the amount of seed ${}^{20}\text{Ne}$ is concurrently affected by processing from the Hot-CNO cycles to the NeNa region through the same reaction sequence discussed above, namely, ${}^{15}\text{O}(\alpha, \gamma){}^{19}\text{Ne}(p, \gamma){}^{20}\text{Na}(p, \gamma){}^{21}\text{Mg}\dots$. Since ${}^{20}\text{Ne}$ is the decay daughter of ${}^{20}\text{Na}$, the importance of the ${}^{20}\text{Na}(p, \gamma){}^{21}\text{Mg}$ reaction in the nova scenario lies in the fact that its rate determines how quickly the ${}^{20}\text{Na}$ is depleted, thereby affecting the subsequent nucleosynthesis in the NeNa cycle.

1.3 Current Knowledge of the Spectroscopy of ${}^{21}\text{Mg}$, and the ${}^{20}\text{Na}(p, \gamma){}^{21}\text{Mg}$ Reaction Rate

As in the case of other reactions in the Hot-CNO cycles and along the breakout paths, the ${}^{20}\text{Na}(p, \gamma){}^{21}\text{Mg}$ ($Q = 3.216$ MeV) reaction is expected to be dominated by contributions from thin and isolated resonances above the ${}^{20}\text{Na} + p$ threshold. While for some reactions, the direct capture to low-lying states may play a significant role, calculations by Wiescher and collaborators [3] indicate that the direct capture contribution to the total ${}^{20}\text{Na}(p, \gamma){}^{21}\text{Mg}$ rate is only marginal in the energy range of interest. Within the resonant rate formalism, the reaction rate $\langle \sigma v \rangle$ as a function of temperature T is given by

$$\langle \sigma v \rangle (T) = \left(\frac{2\pi}{\mu kT} \right)^{3/2} \hbar^2 \sum_i (\omega\gamma)_i \exp\left(-\frac{E_i}{kT}\right), \quad (3)$$

where μ is the reduced mass, $(\omega\gamma)_i$ are the resonance strengths, and E_i are the resonance energies. Thus, given that the direct component can be neglected for our purposes, the ${}^{20}\text{Na}(p, \gamma){}^{21}\text{Mg}$ rate can be determined to an adequate precision once the resonance energies and strengths are known.

With regards to the level structure of ${}^{21}\text{Mg}$ of interest for the ${}^{20}\text{Na}(p, \gamma){}^{21}\text{Mg}$ reaction, our present knowledge is based largely on a study by Kubono and collaborators [4], who populated states in ${}^{21}\text{Mg}$ using the ${}^{24}\text{Mg}({}^3\text{He}, {}^6\text{He}){}^{21}\text{Mg}$ reaction. The resonance energies for the levels that they found were measured to within ± 15 keV, and tentative J^π values were assigned based on DWBA fits to angular distribution data, as well as from comparisons with the structure information available for ${}^{21}\text{F}$, the mirror of ${}^{21}\text{Mg}$. Their conclusions are summarized in the level schemes shown in Figure 2, where the tentative isobaric analogue assignments adopted by Kubono et al. are also displayed. With these mirror assignments, the ${}^{20}\text{Na}(p, \gamma){}^{21}\text{Mg}$ reaction rate was calculated using the resonance parameters listed in Table 1, which includes measured resonance energies, along with resonance strengths and partial widths estimated with information available from previous studies [3,5]. The resulting rate is plotted as a function of temperature in Figure 3, and their results point to a resonance at 131 keV ($E_x = 3.347$ MeV) as the dominant one at the peak temperatures found in novae ($T = 0.1 - 0.3$ GK), while at the higher temperatures characteristic of breakout to the rp-process in x-ray bursts ($T \geq 0.6$ GK), the 536 keV resonance ($E_x = 3.752$ MeV) controls the overall reaction rate.

While the ($^3\text{He}, ^6\text{He}$) study was a significant improvement in our understanding of the $^{20}\text{Na}(p,\gamma)^{21}\text{Mg}$ reaction rate, many of the level parameters required for calculating the rate are not known. In particular, the J^π values derived from the angular distributions are not definite, as seen in Table 1, and the mirror assignments used to determine the J^π and partial widths are also tentative. One should also note that the spins and parities for the mirror states in ^{21}F [5] are not unambiguously determined either. Lastly, since the ($^3\text{He}, ^6\text{He}$) measurement has been the only spectroscopic study on ^{21}Mg so far, the existence of missing states in the important energy region cannot be discounted.

In light of the above, and given the ready availability of a ^{20}Na beam at ISAC following the $^{21}\text{Na}(p,\gamma)^{22}\text{Mg}$ measurement (E824), we propose to measure the strengths of the important resonances directly, thereby placing the $^{20}\text{Na}(p,\gamma)^{21}\text{Mg}$ reaction rate on firmer experimental ground.

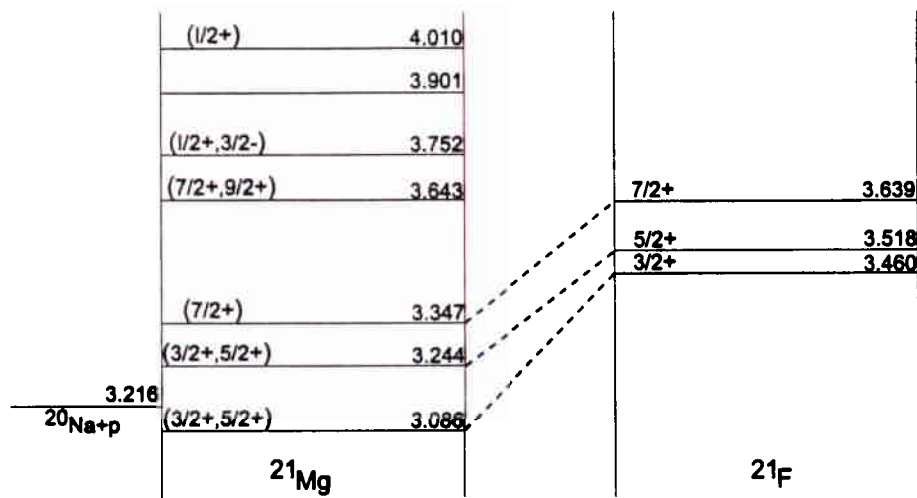


Fig. 2 Level structure of ^{21}Mg and ^{21}F near the $^{20}\text{Na} + p$ threshold.

Table 1 Resonance parameters adopted in Ref. [4] for the $^{20}\text{Na}(p,\gamma)^{21}\text{Mg}$ reaction. The J^π assignments used to calculate the ω_γ values are shown in boldface.

$E_x(^{21}\text{Mg})$ (MeV \pm 15 keV)	E_r (MeV)	J^π	θ^2 ^{a)}	Γ_p ^{b)} (eV)	Γ_γ ^{c)} (eV)	ω_γ (meV)
3.086	-0.130	($3/2^+, 5/2^+$)	0.1		0.188	
3.244	0.028	($3/2^+, 5/2^+$)	0.1	3.04×10^{-19}	.0833	1.82×10^{-16}
3.347	0.131	($7/2^+$)	0.1	1.23×10^{-6}	.274	9.84×10^{-4}
3.643	0.427	($7/2^+, 9/2^+$)	0.1	1.58×10^{-4}	6.09×10^{-3}	6
3.752	0.536	($1/2^-, 3/2^-$)	0.1	99.4	0.1	40
3.901	0.685	($7/2^-$)	0.1	0.872	0.1	70
4.010	0.794	($1/2^+$)	0.1	4720	0.439	88

^{a)} From Ref. [3].

^{b)} From Ref. [4]. Note that the Γ_p for $E_x = 3.643$ MeV state is wrong, since it was calculated in Ref. [4] under the incorrect assumption that the l -value for this state is 4 instead of 2.

^{c)} Inferred from Ref. [5].

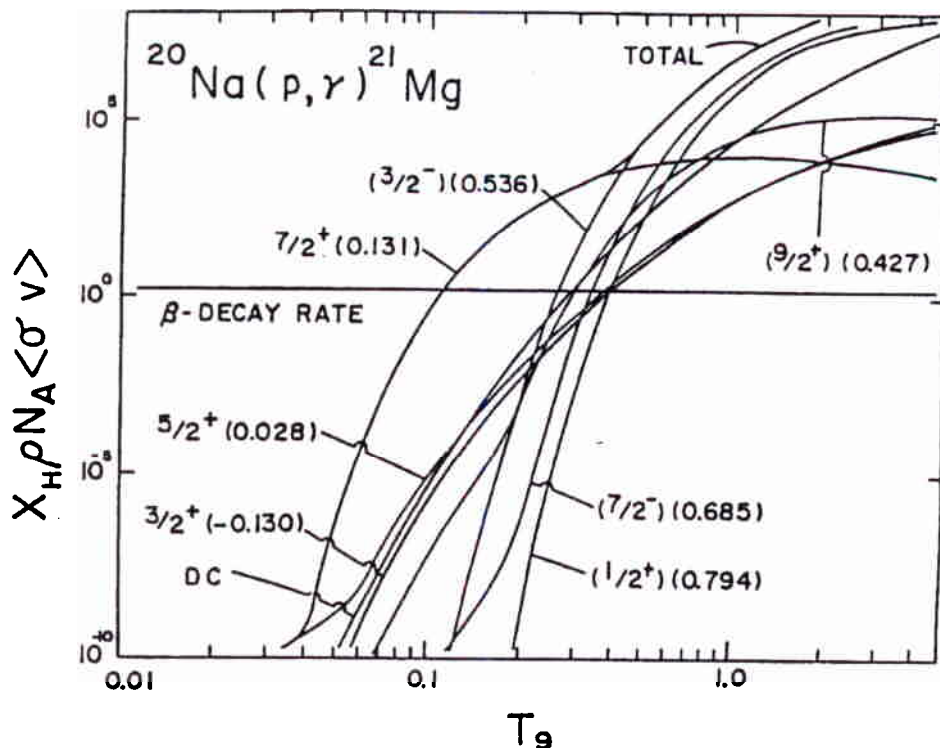


Fig. 3 The $^{20}\text{Na}(p,\gamma)^{21}\text{Mg}$ resonant reaction rate calculated in Ref. [4], plotted as a function of temperature (in GK). The parameters used are given in Table 1; the value of $X_H\rho$ assumed is $5 \times 10^5 \text{ g/cm}^3$ (figure reproduced from Ref. [4]).

2 Experimental Considerations and Plans

The $^{20}\text{Na}(p,\gamma)^{21}\text{Mg}$ reaction will be measured in inverse kinematics with a ^{20}Na beam bombarding a hydrogen target. To avoid uncertainties related to changes in target composition and stability over a run, the target will be a windowless, differentially pumped, hydrogen gas target running in recirculation mode. The target has a length of 10 cm, and at a pressure of 4.5 Torr, the target thickness is approximately $3 \times 10^{18} \text{ atoms/cm}^2$. With this setting, the energy loss of the beam in the target is on the order of 10 keV/cm and therefore large compared to the estimated resonance widths. Thus, the thick target yield formalism can be used to determine the total reaction rate. For a given resonance, the resonance strength $\omega\gamma$ is related to the yield per incoming ion Y through the expression

$$Y = \frac{\lambda^2}{2\epsilon} \frac{M+m}{M} \omega\gamma, \quad (4)$$

where λ^2 is the de Broglie wavelength of a particle with a mass corresponding to the reduced mass of the entrance channel and with an energy equal to the centre of mass energy of the system. M is the target mass, m is the projectile mass, and ϵ is the beam energy loss per atom per unit area within a target of density n , given by $\epsilon = \frac{1}{n} \frac{dE}{dx}$.

Table 2 lists experimental parameters for the important $^{20}\text{Na} + p$ resonances. The

column labeled E_r gives the resonance energies from Ref. [4] in both the centre-of-mass frame (cm) and the lab system (lab). E_{beam}/A is the energy of the beam per unit mass that is needed to place the resonance at the target center; ΔE is the energy loss in the target calculated with SRIM, while σ_{beam} is the beam energy spread, assumed to be 0.2%. The half opening angle for the ^{21}Mg recoils, $\Delta\theta$, was determined for a ground state gamma transition. Lastly, the production rates were estimated assuming a ^{20}Na beam intensity of 10^{10} particles/s, a probability of 40% for the selected charge state, and 100% transmission through the DRAGON separator.

Table 2 Experimental parameters for the three important $^{20}\text{Na}(p,\gamma)^{21}\text{Mg}$ resonances, as seen in the centre-of-mass (cm) and lab frames.

ref. frame	E_r (keV)	E_{beam}/A (MeV/u)	ΔE (keV/cm)	σ_{beam} (keV)	$\Delta\theta$ (deg.)	Yield per ion	Prod. rate(cph)
cm	131			0.14			
lab	2751	0.141	12.7	2.8	0.6	1.6×10^{-14}	0.23
cm	427			0.45			
lab	8967	0.452	14.6	9.0	0.36	2.6×10^{-11}	378
cm	536			0.57			
lab	11256	0.566	14.5	11.3	0.33	1.4×10^{-10}	2060

The estimated count rates in Table 2 show that the strengths of the 427 keV and 536 keV resonances are measurable to at least 20% accuracy. On the other hand, a measurement of the 131 keV resonance with high statistics will likely be hampered because its estimated resonance strength is extremely low, and the beam energy required is just below the nominal limit (150 keV/u) of the ISAC accelerator. However, beams of lower energy but probably poorer quality might be possible [6]. A better understanding of the capabilities of the ISAC accelerator will be available upon its commissioning.

From the astrophysics point of view, the 131 keV resonance will play a negligible role in x-ray burst scenarios, where the Gamow energy window is at $E_x = 3.638 \pm 0.17$ MeV for $T = 0.6$ GK. However, this resonance may be important at the lower temperatures found in novae, and therefore, at the very least, we plan to determine an upper limit on its resonance strength.

3 Experimental Equipment

3.1 ISAC and the DRAGON Facility

The ^{20}Na beam will be produced in an on-line source using the ISOL method. The ions of interest are separated in a high resolution ($\Delta M/M = 1/10000$) mass analyzer and accelerated by a 35 MHz radio frequency quadrupole (RFQ), which is designed for beams with a ratio $1/30 \leq q/A \leq 1/6$. A medium energy beam transport (MEBT) system strips the beam to $1/6 \leq q/A \leq 1/3$ before it reaches a final energy of 0.15 to 1.5 MeV/u at the

end of a drift tube linac (DTL). Bunchers provide a pulsed structure and maintain a low energy spread of less than 0.2%. Stable beams of ^{20}Ne and ^{21}Ne for calibration purposes will be produced from an off-line ion source.

The DRAGON (Detector of Recoils And Gammas Of Nuclear reactions) facility has been optimally designed to measure alpha- and proton-capture reactions in inverse kinematics using heavy-ion beams incident on a gas target of hydrogen or helium. DRAGON (see Fig. 4) is presently under construction, and is comprised of a differentially pumped, windowless gas target (including an array of BGO gamma-ray detectors), a state-of-the-art electromagnetic mass separator (EMS), and an assembly of focal plane detectors. For a more detailed description of the DRAGON facility, the reader is referred to Ref. [7]. The use of DRAGON to measure the $^{20}\text{Na}(p,\gamma)^{21}\text{Mg}$ reaction rate, generally speaking, will be very similar to that proposed for the measurement of the rate (E824), delineated in Ref. [8].

The EMS will accomplish most of the separation of the capture products from the beam particles that pass through the target. The entrance acceptance of the DRAGON EMS is sufficiently large to accommodate the ^{21}Mg recoils from the three important resonances. Since the momentum of the recoils and the contaminant beam particles are nearly identical, a separation based on their mass difference is required, leading to the use of a combination of magnetic and electrostatic dipoles. A beam suppression factor of at least 10^{10} is expected before the ions reach the final focus at the end-detector assembly, where an additional suppression of 100 is anticipated.

The recoiling ^{21}Mg are identified and separated from the ^{20}Na beam particles at the final focus through measurements of their time-of-flight over a path of 50 cm, and of their total energy. Different detector configurations are available, using a combination of microchannel plates detectors, solid state detectors and/or an ionization chamber with a parallel grid avalanche counter, depending on the requirements of the experiment. A more comprehensive description of the end-detector assembly is given in Ref. [8].

3.2 Measurement of Background

In order to attain the highest possible accuracy in our measurement, an understanding of the expected background is required. If the BGO gamma array is functional by the time the experiment is ready to begin, the measurement of coincidences between the events at the end-detector assembly and the prompt gamma-ray signals will suppress most of the possible background events. If the gamma array is unavailable, then any A=21 contamination cannot be distinguished from the recoils of interest, regardless of whether the contaminant is present in the beam coming out of the source, or produced by a reaction in the gas target. However, since the first stage of the accelerator is followed by a high resolution mass analyzer ($\Delta M/M = 1/10000$), a contamination in the beam of A=21 isotopes is not expected, but should however be checked in advance with the Z-discrimination capability of the ionization chamber located at the final focus.

A more probable source of background would be events from (p,γ) reactions in the target on A=20 contamination in the beam. The most important of these potentially interfering reactions is $^{20}\text{Ne}(p,\gamma)^{21}\text{Na}$, even though the ^{20}Ne component in the beam should be very small since ^{20}Ne , as a noble gas isotope, is significantly harder to ionize

than ^{20}Na . Moreover, since the mass difference between ^{20}Ne and ^{20}Na is about 1:1500, the ISAC mass analyzer should provide further discrimination against ^{20}Ne before the beam reaches the gas target. Even if the ^{20}Ne beam contaminants do reach the target, they will have a low cross-section for a (p,γ) reaction, and in any case, one should note that there are no known resonances for $^{20}\text{Ne}(p,\gamma)^{21}\text{Na}$ in the energy region that we will be probing in the $^{20}\text{Na}(p,\gamma)^{21}\text{Mg}$ reaction study [9].

Lastly, in order to ensure that the potential contribution from the (d,n) channel due to deuterium contamination in the gas target is understood, we will measure the $^{20}\text{Na}(d,n)^{21}\text{Mg}$ reaction with the ^{20}Na beam, using a deuterated polyethelene foil to avoid contaminating the gas target cell.

4 Readiness

If approved, the $^{20}\text{Na}(p,\gamma)^{21}\text{Mg}$ measurement will likely be scheduled to be performed after the measurement of the $^{21}\text{Na}(p,\gamma)^{22}\text{Mg}$ reaction rate (E824), and therefore by then the DRAGON facility will be fully commissioned. Additionally, the development of high-quality beams of these Na isotopes will have been completed. Furthermore, since the charge state distribution of the Mg recoils will have been measured prior to running E824, no further distribution measurements will be required for the $^{20}\text{Na}(p,\gamma)^{21}\text{Mg}$ reaction study. Hence, once E824 is completed, we will be ready to start the $^{20}\text{Na}(p,\gamma)^{21}\text{Mg}$ experiment without any anticipated delays.

5 Beam Time Required

Our beam time requirements are listed below, and include time for measurements of contributions from the higher resonances at 685 keV and and 794 keV:

Measurement:	Shifts Required:
- DRAGON calibration with stable beams	10
- Resonance at 427 keV	2
- Resonance at 536 keV	1
- Resonances at 685 and 794 keV	1
- Upper limit for 131 keV resonance	10
- Off-resonance runs	20
- Background measurement	5
- Contingency	5
TOTAL	54 shifts

Table 3 Estimated beam time requirements for the $^{20}\text{Na}(p,\gamma)^{21}\text{Mg}$ study.

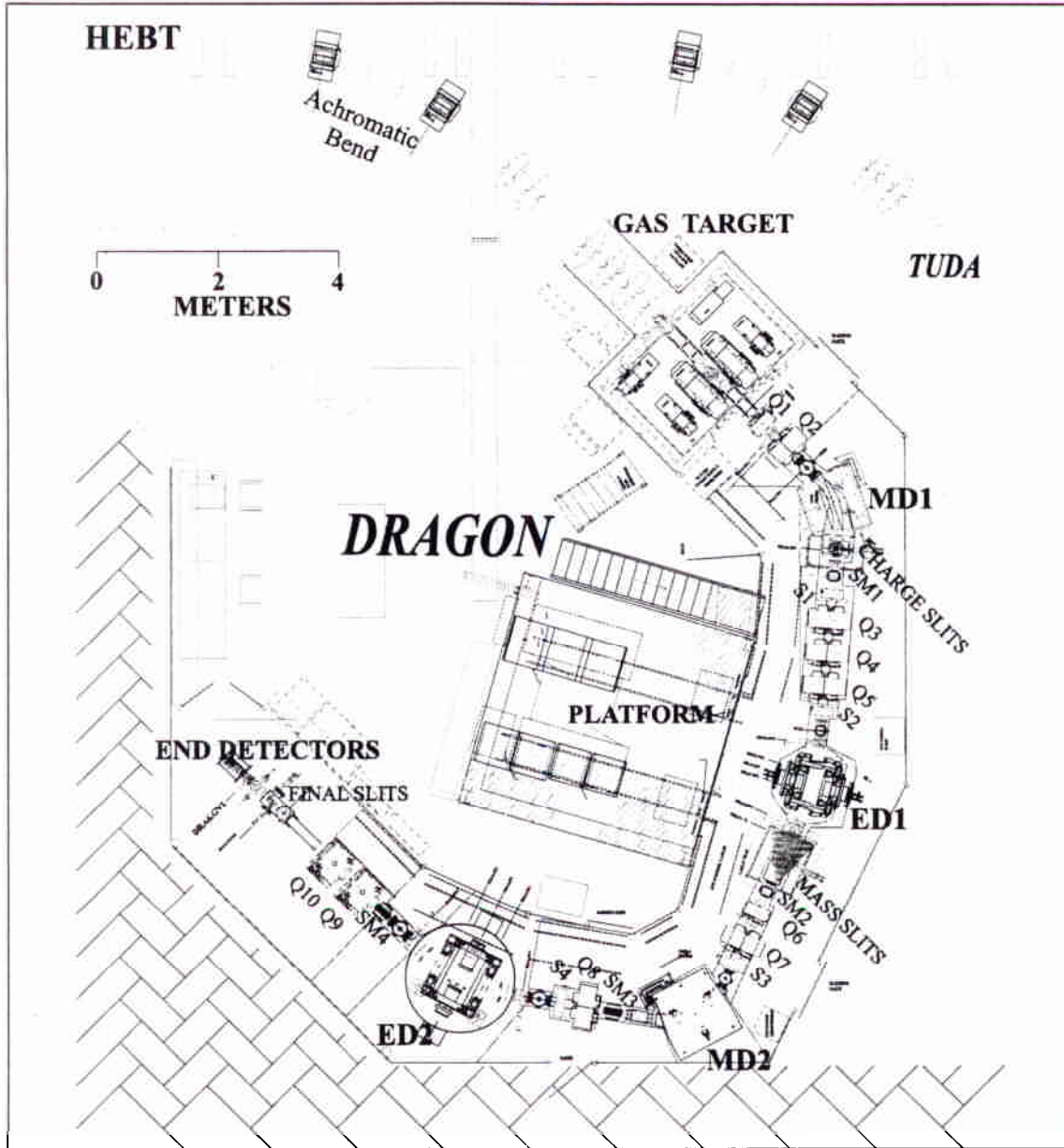


Fig. 4 The DRAGON facility. The four major components are shown: the windowless gas target, the gamma detector array, the EMS (composed of two magnetic dipoles and two electrostatic benders) and the recoil end-detector station.

References

1. M. Wiescher, H. Schatz and A.E. Champagne, *Phil. Trans. R. Soc. Lond. A* **356** 2105 (1998).
2. M. Wiescher, J. Görres, and H. Schatz, *Journal of Physics G* **25** 133 (1999).
3. M. Wiescher, J. Görres, F.K. Thielemann and H. Ritter, *Astron. & Astrophys.* **160** 56 (1986).
4. S. Kubono et al., *Nucl. Phys.* **A537** 153 (1992).
5. D.E. Alburger et al., *Phys. Rev. C* **23**, 2217 (1981).
6. Robert Laxdal estimates that ^{20}Na beams as low as 129 keV/u are possible; private communication (2000).
7. NSERC Major Installation Grant Report for DRAGON (1997).
8. J.M. D'Auria et al., E824 proposal approved by the TRIUMF EEC (1997).
9. P.M. Endt, *Nucl. Phys.* **A521** 1 (1990).

Include publications in refereed journal over at least the previous 5 years.

1. Bateman, N., K. Abe, G. Ball, L. Buchmann, J. Chow, J.M. D'Auria, Y. Fuchi, C. Iliadis, H. Ishiyama, K.P. Jackson, S. Karataglidis, S. Kato, et al., "Measurement of the $^{24}\text{Mg}(p,t)^{22}\text{Mg}$ Reaction and Implications for the $^{21}\text{Na}(p,\gamma)^{22}\text{Mg}$ Stellar Reaction Rate," to be published in Phys. Rev. C.
2. D'Auria, J.M. for the DRAGON Collaboration, "Astrophysics with a DRAGON at ISAC," to be published in Nucl. Phys. A.
3. D'Auria, J.M., "Radioactive Beams: A Probe for Atoms and Nuclei," J. of Radioanalytical and Nucl. Chem. 243 1 59 (2000).
4. Gete, E., L. Buchmann, R.E. Azuma, D. Anthony, N. Bateman, J.C. Chow, J.M. D'Auria, M. Dombisky, U. Giesen, C. Iliadis, K.P. Jackson, J.D. King, D.F. Measday and A.C. Morton, "The β -delayed Particle Decay of ^9C and the $A=9$, $T=1/2$ Nuclear System: 1. Experiment, Data and Phenomenological Analysis," Phys. Rev. C 61 064310 (2000).
5. Lange, R., J. D'Auria, U. Giesen, J. Vincent and T. Ruth, "Preparation of a Radioactive ^{44}Ti Target," Nucl. Instr. Meth. A423 247 (1999).
6. Chow, J.C., A.C. Morton, R.E. Azuma, N. Bateman, R.N. Boyd, L. Buchmann, J.M. D'Auria, T. Davinson, M. Dombisky, W. Galster, E. Gete, U. Giesen, C. Iliadis, K.P. Jackson, J.D. King, G. Roy, T. Shoppa, and A. Shotter, "Three Particle Break-Up of the Isobaric Analog State in ^{17}F ," Phys. Rev. C57 2 R475 (1998).
7. D'Auria, J.M., J. Behr, L. Buchmann, M. Dombisky, K.P. Jackson and H. Sprenger, "The TISOL Facility at TRIUMF: Operational Status at 10 Years," Nucl. Instr. Meth. B126 7 (1997).
8. D'Auria, J.M., L. Buchmann, D. Hutcheon, P. Lipnik, D. Hunter, J. Rogers, R. Helmer, U. Giesen, A. Olin, P. Bricault and N. Bateman, "A Facility for Studying Radiative Capture Reactions Induced with Radioactive Beams at ISAC," Nucl. Instr. Meth. B126 262 (1997).
9. Behr, J., A. Gorelov, T. Swanson, O. Husser, K.P. Jackson, M. Trinczek, U. Giesen, J.M. D'Auria, R. Hardy, T. Wilson, P. Chobotov, F. LeBlond, L. Buchmann, M. Dombisky, C.D.P. Levy, G. Roy, B.A. Brown and J. Dilling, "Magneto-optic Trapping of β -Decaying $^{38}\text{K}^m$, ^{37}K from an On-Line Isotope Separator," Phys. Rev. Lett. 79 375 (1997).
10. King, J.D., R.E. Azuma, C. Iliadis, A.C. Morton, L. Buchmann, M. Dombisky, K.P. Jackson, J.M. D'Auria, U. Giesen, G. Roy, T. Davinson, A. Shotter, W. Galster and R.N. Boyd, "Investigation of the $^{12}\text{C}(\alpha,\gamma)^{16}\text{O}$ Reaction via the β -delayed Proton Decay of the ^{17}Ne ," Nucl. Phys. A621 169 (1997).
11. Iliadis, C., R.E. Azuma, J. Chow, J.D. King, A.C. Morton, L. Buchmann, M. Dombisky, K.P. Jackson, J.M. D'Auria, U. Giesen, J.G. Ross, H. Schatz and M. Wiescher, "Decay Studies of Importance to Explosive Hydrogen Burning," Nucl. Phys. A621 211 (1997).

12. D'Auria, J.M., L. Buchmann, D. Hutcheon, P. Lipnik, D. Hunter, J. Rogers, R. Helmer, U. Giesen, A. Olin and P. Bricault, "A Facility for Studying Radiative Capture Reactions Induced with Radioactive Beams at ISAC," Nucl. Phys. A621 599 (1997).
13. Iliadis, C., R.E. Azuma, L. Buchmann, J. Chow, J.M. D'Auria, M. Dombisky, U. Giesen, J.D. King and A.C. Morton, "Beta-delayed Particle Decay of ^{36}K ," Nucl. Phys. A609 237 (1996).
14. James, M., J. Bailey and J.M. D'Auria, "A Volcanic Glass Library for the Pacific Northwest: Problems and Prospects," Can. J. of Archaeology 20 93 (1996).
15. D'Auria, J.M., "A Review of Radioactive Beam Facilities in the World," Nucl. Instr. Meth. B99 330 (1995).
16. A.A. Chen, R. Lewis, K.B. Swartz, P.D. Parker, and D.W. Visser, "The Structure of ^{22}Mg and its Implications for Explosive Nucleosynthesis," to be published in Physical Review C.
17. A.A. Chen, R. Lewis, K.B. Swartz, P.D. Parker, and D.W. Visser, "Explosive Nucleosynthesis and the Structure of ^{22}Mg ," to be published in the Proceedings of the 6th International Conference on Nuclei in the Cosmos, Nuclear Physics A.
18. J.C. Blackmon, D.W. Bardayan, W. Bradfield-Smith, A.E. Champagne, A.A. Chen, T. Davinson, K.I. Hahn, R.L. Kozub, Z. Ma, P.D. Parker, G. Rajbaidya, R.C. Runkle, C.M. Rowland, A.C. Shotter, M.S. Smith, K.B. Swartz, D.W. Visser and P.J. Woods, "Measurement of the $^1\text{H}(^{17}\text{F}, \alpha)^{14}\text{O}$ Cross Section and the $^{14}\text{O}(\alpha, p)^{17}\text{F}_{g.s.}$ Reaction Rate," to be published in the Proceedings of the 6th International Conference on Nuclei in the Cosmos, Nuclear Physics A.
19. D.W. Bardayan, J.C. Blackmon, C.R. Brune, A.E. Champagne, A.A. Chen, J.M. Cox, T. Davinson, V.Y. Hansper, M.A. Hofstee, B.A. Johnson, R.L. Kozub, Z. Ma, P.D. Parker, D.E. Pierce, M.T. Rabban, A.C. Shotter, M.S. Smith, K.B. Swartz, D.W. Visser, and P.J. Woods, "The Astrophysically Important 3^+ State in ^{18}Ne and the $^{17}\text{F}(p, \gamma)^{18}\text{Ne}$ Stellar Rate," Physical Review C 62, 055804 (2000).
20. D.W. Bardayan, J.C. Blackmon, C.R. Brune, A.E. Champagne, A.A. Chen, J.M. Cox, T. Davinson, V.Y. Hansper, M.A. Hofstee, B.A. Johnson, R.L. Kozub, Z. Ma, P.D. Parker, D.E. Pierce, M.T. Rabban, A.C. Shotter, M.S. Smith, K.B. Swartz, D.W. Visser, and P.J. Woods, "Observation of the Astrophysically Important 3^+ State in ^{18}Ne via Elastic Scattering of a Radioactive ^{17}F Beam from ^1H ," Physical Review Letters 83 1, 45 (1999).
21. B. Harss, J.P. Greene, D. Henderson, R.V.F. Janssens, C.L. Jiang, J. Nolen, R.C. Pardo, K.E. Rehm, J.P. Schiffer, R.H. Siemssen, A.A. Sonzogni, J. Uusitalo, I. Wiedenhöver, M. Paul, T.F. Wang, F. Borasi, R.E. Segel, J.C. Blackmon, M.S. Smith, A. Chen, P. Parker, "Stellar Reactions with Short-Lived Nuclei: $^{17}\text{F}(p, \alpha)^{14}\text{O}$," Physical Review Letters 82 20, 3964 (1999).
22. K.O. Yildiz, N.P.T. Bateman, Y.M. Butt, A.A. Chen, K.B. Swartz, P.D. Parker, "Thick Target Yields of $^{26}\text{Al}_{g.s.}$ from the $^{16}\text{O}(^{16}\text{O}, x)^{26}\text{Al}_{g.s.}$ and $^{16}\text{O}(^{14}\text{N}, x)^{26}\text{Al}_{g.s.}$ Reactions," Physical Review C 60, 028801 (1999).

23. N.P.T. Bateman, D.W. Bardayan, Y.M. Butt, A.A. Chen, K.O. Yildiz, B.M. Young, P.D. Parker, "Thick Target Yield of ^{26}Al from the $^{12}\text{C}(^{16}\text{O}, x)^{26}\text{Al}_{g.s.}$ Reaction," *Physical Review C* 57 4, 2022 (1998).
24. S. Utku, J.G. Ross, N.P.T. Bateman, D.W. Bardayan, A.A. Chen, J. Görres, A.J. Howard, C. Iliadis, P.D. Parker, M.S. Smith, R.B. Vogelaar, M. Wiescher, K. Yildiz, "Breakout from the Hot CNO Cycle: The $^{18}\text{F}(p, \gamma)$ vs. $^{18}\text{F}(p, \alpha)$ Branching Ratio," *Physical Review C* 57 5, 2731 (1998).
25. N.P.T. Bateman, D.W. Bardayan, Y.M. Butt, A.A. Chen, K.O. Yildiz, B.M. Young, P.D. Parker, A.E. Champagne, "The Production of ^{26}Al in the Early Solar System by Oxygen Rich Cosmic Rays," *Proceedings of the 4th International Conference on Nuclei in the Cosmos, Nuclear Physics A621 60c-63c*, eds. J. Grres, G. Mathews, S. Shore, M. Wiescher (1997).
26. L. Buchmann, R.E. Azuma, C.A. Barnes, A. Chen, J. Chen, J.M. D'Auria, M. Dombisky, U. Giesen, K.P. Jackson, J.D. King, R. Korteling, P. McNeely, J. Powell, G. Roy, M. Trinczek, J. Vincent, P.R. Wrean, S.S.M. Wong, "The β -delayed α Spectrum of ^{16}N and the Low-energy Extrapolation of the $^{12}\text{C}(\alpha, \gamma)^{16}\text{O}$ Cross Section," *Proceedings of the 2nd International Conference on Nuclei in the Cosmos, Journal of Physics G: Nuclear and Particle Physics* 19 S115-S126 (1993).